



Kinetic energy partitions in electron–ion PIC simulations of ABC fields

Qiang Chen

Abstract. We explore the kinetic energy partitions between electrons and ions in the 2-D magnetostatic equilibria called Arnold–Beltrami–Childress (ABC) fields, using particle-in-cell (PIC) numerical simulations. We cover a wider range of ion–electron temperature combinations and get different results compared to previous studies of the Harris-layer-type magnetic reconnection simulations. We find that the initial ion–electron enthalpy ratio is an important indicator. The particle species that dominates the total enthalpy will also dominate the kinetic energy gains and the momentum distribution peaks, but the other species have higher nonthermal energy fractions because both species show similar maximum energies.

Keywords: Acceleration of particles • Magnetic reconnection • Relativistic processes • Simulations

Introduction

Various astrophysical environments involve extremely rapid and very luminous gamma-ray flares, such as the blazars and the Crab pulsar wind nebula (PWN). Particle acceleration mechanisms are needed to explain how magnetic energy is released and converted to kinetic energy. Currently, magnetic reconnection is one of the very promising candidates (for a review, see references [1, 2]).

The essential condition for triggering magnetic reconnection includes oppositely directed magnetic fields and a very thin current sheet that can be produced by certain plasma instabilities. The traditional magnetic field configuration is the Harris-layer-type kinetic equilibrium [3], in which the kinetic-scale current layer limits the outflow (reconnection rate) to the order of $\partial(0.1)$; hence, the magnetic dissipation efficiency is also limited. In order to understand the rapid and efficient conversion of electromagnetic energy into radiation, the Arnold–Beltrami–Childress (ABC) fields [4, 5] have recently been proposed as an alternative candidate [6–8].

Owing to the improvements in computational power, we can study the properties of magnetic reconnection by practicing numerical simulation. Based on the ABC fields, we particularly focus on the difference in the behaviors of electrons and ions, especially their kinetic energy gains.

Q. Chen
Nicolaus Copernicus Astronomical Center, Polish
Academy of Sciences
Bartycka 18 St., 00-716 Warsaw, Poland
and Institute of Plasma Physics and Laser Microfusion
Hery 23 St., 01-497 Warsaw, Poland
E-mail: qchen.astro@gmail.com

Received: 15 July 2022

Accepted: 18 November 2022

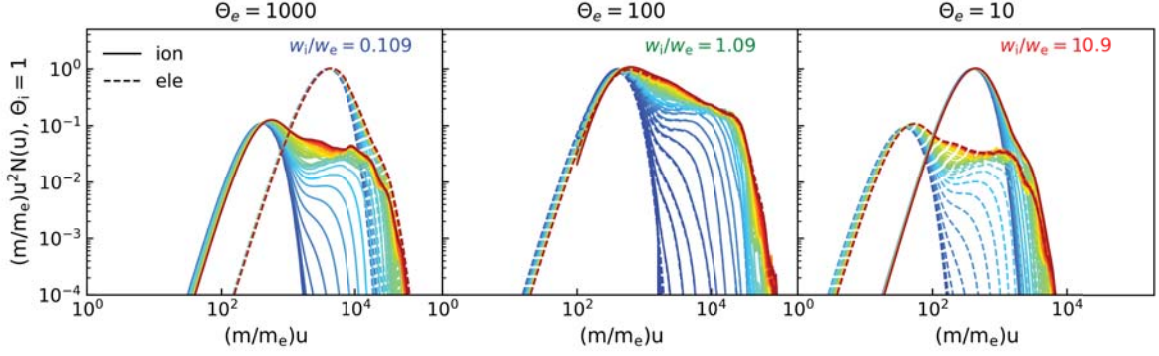


Fig. 1. Particle momentum distributions of three chosen typical simulations, for $\mu = 100$, $\tilde{a}_1 = 0.25$, and the size = 4608^2 cells. The initial enthalpy ratio w_i/w_e is indicated in each panel with a different color, so as to make it easier to compare with Fig. 2.

Simulation setup

We performed particle-in-cell (PIC) numerical simulations using the Zeltron code⁽¹⁾ [9] of 2-D periodic magnetic equilibria known as the ABC fields [10–12]:

$$(1) \quad \begin{aligned} B_x &= B_1 [\sin(\alpha_0(x+y)) + \sin(\alpha_0(x-y))] / \sqrt{2} \\ B_y &= B_0 [\sin(\alpha_0(x-y)) - \sin(\alpha_0(x+y))] / \sqrt{2} \\ B_z &= B_0 [\cos(\alpha_0(x+y)) - \cos(\alpha_0(x-y))] \end{aligned}$$

where $\alpha_0 = 2\pi k_{\text{eff}}/L$ for the linear domain size L and $k_{\text{eff}} = \sqrt{2}$ is the effective wavenumber.

The particle density is given by the expression

$$(2) \quad n = \frac{3\sqrt{2}\alpha_0 B_0}{4\pi e\tilde{a}_1 \langle \beta \rangle}$$

where $\langle \beta \rangle$ is the average dimensionless speed of ions and electrons, and $\tilde{a}_1 \leq 1/2$ is a constant that normalizes the dipole moment of the local particle distribution. The initial total mean magnetization is given as follows:

$$(3) \quad \langle \sigma_{\text{ini}} \rangle = \frac{2\sqrt{2}\tilde{a}_1 \langle \beta \rangle}{3[C_{w,i}(\Theta_i)\mu + C_{w,e}(\Theta_e)]\alpha_0 \rho_e}$$

where $C_w(\Theta) = 4\Theta + K_1(1/\Theta)/K_2(1/\Theta)$ is a function of the dimensionless temperature $\Theta = kT/mc^2$ and $K_n(x)$ is the modified Bessel function of the second kind with $n = 0, 1, 2$. In this paper, we use the subscript “i” to represent the parameters related to ions and “e” to represent electrons. Further, $\rho_e = m_e c^2 / eB_0$ is the electron gyroradius.

We investigate a wide range of relativistic ion temperatures as $10^{-2} \leq \Theta_i \leq 10^2$ and electron temperatures as $10^{-2} \leq \Theta_e \leq 10^5$. We set $B_0 = 1$. In order to resolve the degeneration of $\langle \sigma_{\text{ini}} \rangle$ with the temperatures Θ_i and Θ_e , we probe \tilde{a}_1 as 0.1, 0.25 (default), and 0.4. We use numerical grids of 2000² and 4608² cells. The particle number per cell per species is 64. The domain size is $L = 1920\rho_0$, where $\rho_0 = \min[\Theta_e m_e c^2 / (eB_0), \mu\Theta_i m_e c^2 / (eB_0)]$ is the nominal gyroradius. Each simulation runs at least 51 000 numerical steps.

For kinetic simulations, it is necessary to resolve the gyroradii of both ions and electrons at the same

time. Limited by the grid sizes and resolutions of both species of particles, we choose mass ratios of $\mu = 10, 100$ instead of the real ion:electron mass ratio 1836. Previous studies configured with mass ratios either as 1836 [13] or a sequence such as 10, 25, 50, and 1836 [14]. Differences caused by the choices of the mass ratio can be ignored by simultaneously increasing the electron temperatures, because the plasma magnetization $\langle \sigma_{\text{ini}} \rangle \propto \Theta_e / \mu$ in the limit $\Theta_e \gg 1$.

In conclusion, our configurations yield initial plasma magnetization $\langle \sigma_{\text{ini}} \rangle \leq 14.38$.

Results

Particle momentum distributions

In Fig. 1, we present the particle momentum distributions $u^2 N(u)$, where u is the dimensionless particle momentum and $N(u)$ is the particle distribution. The momentum distributions are multiplied with the mass ratio m/m_e , where m represents the mass of either the ions or the electrons accordingly. We did up to 50 runs of simulations, but here, we only present three representative simulations based on the value of the initial enthalpy ratio w_i/w_e , i.e., whether the enthalpy is ion-dominated, electron-dominated, or equivalently dominated. We find that the question of which particle species dominates in the initial stage is very important, because the peaks of the spectra are directly related to the initial enthalpy ratio. The particle species that dominates the initial enthalpy produces a higher spectral peak.

Nonthermal fraction evolutions

However, Fig. 2 shows that the other species dominates both the nonthermal particle number and the energy fractions, and both species reach a similar level of the maximum particle energy γ_{max} (Lorentz factor).

Kinetic energy partitions

In Fig. 3, we show the kinetic energy partition between ions and electrons. We find that a significant part of our results does not agree with those

⁽¹⁾ <http://benoit.cerutti.free.fr/Zeltron/>.

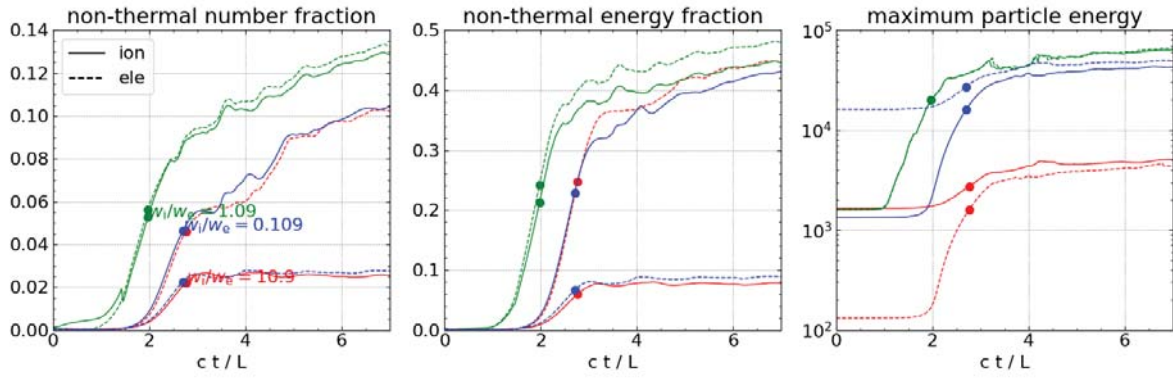


Fig. 2. Nonthermal number fraction, nonthermal energy fraction, and maximum particle energy γ_{\max} for the cases shown in Fig. 1.

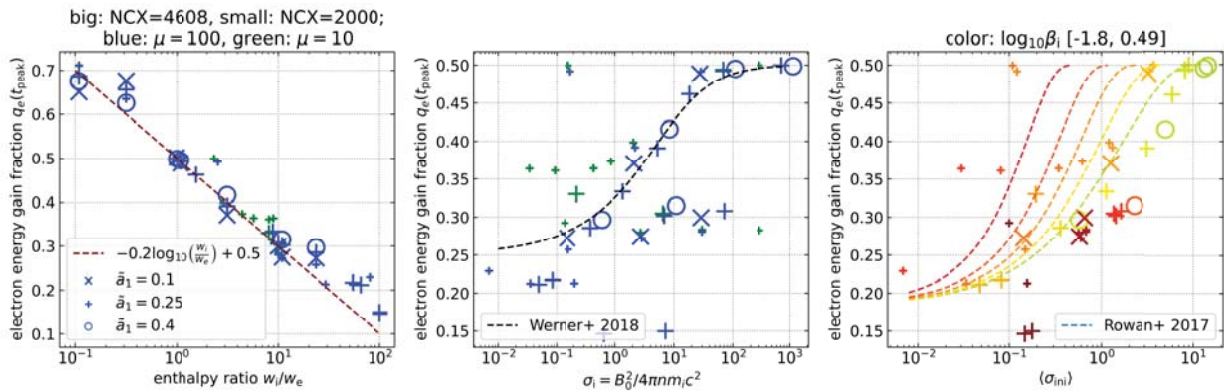


Fig. 3. The left panel shows the dependence of q_e on the initial enthalpy ratio w_i/w_e . The middle and right panels compare the relative gains q_e of the electron’s kinetic energies with the results of previous studies (dashed lines). The marker styles and colors are indicated in the figure.

of previous studies [13, 14]. Our results show that the energy partition is strongly connected with the initial enthalpy ratio w_i/w_e instead of the initial ion cold magnetization $\sigma_i = B_0^2/4\pi n m_i c^2$ or the initial total hot magnetization $\langle \sigma_{\text{ini}} \rangle$, such that the species dominating the initial enthalpy also dominates the kinetic partition.


Conclusion

In this contribution, we show that the initial ion–electron enthalpy ratio determines the partition of kinetic energy between the particle species, such that the species dominating the initial enthalpy also dominates the peak of the spectra and the kinetic energy gains. However, because both species reach a similar level of the maximum particle energy by the end of the simulations, the species not dominating the initial enthalpy dominates the nonthermal particle number fractions and the nonthermal energy fractions. These results differ from the findings of previous studies, because not all our results follow their predicted trends. One most likely reason is that the majority of the previous papers’ choices of the ion–electron temperature combinations are limited in or near the relation $\Theta_i = \Theta_e/\mu$, but the cases other than this relation are not taken into consideration. On the other hand, our results cover relatively larger temperature combinations. Meanwhile, we are currently analyzing whether these differences

may also result from using different initial magnetic field configurations.

Acknowledgments. Thank Dr. Krzysztof Nalewajko, Prof. Dr. Ryszard Miklaszewski and the reviewer for discussions or comments. Thank Dr. Ewa Łaszyńska and the Kudowa Summer School for helps. Our simulations were performed at the Prometheus located at the AGH University of Science and Technology in Krakow, Poland, and at the Chuck located at the Nicolaus Copernicus Astronomical Center of the Polish Academy of Sciences in Warsaw, Poland. This work was supported by the Polish National Science Center through grant numbers 2015/18/E/ST9/00580 and 2021/41/B/ST9/04306.

ORCID

Q. Chen  <http://orcid.org/0000-0002-0547-1544>

References

1. Uzdensky, D. A. (2011). Magnetic reconnection in extreme astrophysical environments. *Space Sci. Rev.*, 160, 45. DOI: 10.1007/s11214-011-9744-5.
2. Yamada, M., Kulsrud, R., & Ji, H. (2010). Magnetic reconnection. *Rev. Mod. Phys.*, 82, 603. DOI: 10.1103/RevModPhys.82.603.

3. Harris, E. G. (1962). On a plasma sheath separating regions of oppositely directed magnetic field. *Il Nuovo Cimento*, 23, 115. DOI: 10.1007/BF02733547.
4. Arnold, V. (1965). Sur une propri tes topologique des applications globalment canonique de la mecanique classique. *CR. Acad. Sci. Paris*, 261, 3719.
5. Dombre, T., Frisch, U., Greene, J. M., H non, M., Mehr, A., & Soward, A. M. (1986). Chaotic streamlines in the ABC flows. *J. Fluid Mech.*, 167, 353. DOI: 10.1017/S0022112086002859.
6. Lyutikov, M., Sironi, L., Komissarov, S. S., & Porth, O. (2017). Explosive X-point collapse in relativistic magnetically dominated plasma. *J. Plasma Phys.*, 83(6), 635830601. DOI: 10.1017/S0022377817000629.
7. Lyutikov, M., Sironi, L., Komissarov, S. S., & Porth, O. (2017). Particle acceleration in relativistic magnetic flux-merging events. *J. Plasma Phys.*, 83(6), 635830602. DOI: 10.1017/S002237781700071X.
8. Lyutikov, M., Komissarov, S., Sironi, L., & Porth, O. (2018). Particle acceleration in explosive relativistic reconnection events and Crab Nebula gamma-ray flares. *J. Plasma Phys.*, 84(2), 635840201. DOI: 10.1017/S0022377818000168.
9. Cerutti, B., Werner, G. R., Uzdensky, D. A., & Begelman, M. C. (2013). Simulations of particle acceleration beyond the classical synchrotron burnoff limit in magnetic reconnection: an explanation of the Crab flares. *Astrophys. J.*, 770, 147. DOI: 10.1088/0004-637x/770/2/147.
10. Chen, Q., Nalewajko, K., & Mishra, B. (2021). Scaling of magnetic dissipation and particle acceleration in ABC fields. *J. Plasma Phys.*, 87, 905870224. DOI: 10.1017/S0022377821000209.
11. Nalewajko, K., Zrake, J., Yuan, Y., East, W. E., & Blandford R. D. (2016). Kinetic simulations of the lowest-order unstable mode of relativistic magnetostatic equilibria. *Astrophys. J.*, 826, 115. DOI: 10.3847/0004-637x/826/2/115.
12. Yuan, Y., Nalewajko, K., Zrake, J., East, W. E., & Blandford, R. D. (2016). Kinetic study of radiation-reaction-limited particle acceleration during the relaxation of unstable force-free equilibria. *Astrophys. J.*, 828, 92. DOI: 10.3847/0004-637x/828/2/92.
13. Werner, G. R., Uzdensky, D. A., Begelman, M. C., Cerutti, B., & Nalewajko, K. (2018). Non-thermal particle acceleration in collisionless relativistic electron-proton reconnection. *Mon. Not. Roy. Astron. Soc.*, 473, 4840. DOI: 10.1093/mnras/stx2530.
14. Rowan, M. E., Sironi, L., & Narayan, R. (2017). Electron and proton heating in transrelativistic magnetic reconnection. *Astrophys. J.*, 850, 29. DOI: 10.3847/1538-4357/aa9380.